PERGAMON International Journal of Mechanical Sciences 43 (2001) 1107–1121

International Journal of MECHANICAL SCIENCES

www.elsevier.com/locate/ijmecsci

Difference in subsurface damage in indented specimens with and without bonding layer

Hadi Helbawi, Liangchi Zhang*, Irena Zarudi

Department of Mechanical and Aeronautical Engineering, The University of Sydney, NSW 2006, Australia

Received 5 July 1999; received in revised form 29 February 2000

Abstract

This paper aims to assess the applicability of the bonded–interface technique (BIT) that has been used for examining sub-surface damage in brittle materials. With the aid of the finite element method, the indentation stress fields in alumina specimens with and without a bonded–interface were analysed. It was found that the bonded–interface greatly alters the stress distribution in the neighbourhood of the interface. The high-stress zone shifts away from the interface, and extends to the surface. Both glue layer mechanical properties and bond thickness play a limited role in the overall stress field of the BIT alumina. Comparisons of theoretical predictions with experimental observations showed that, to a great extent, the BIT presents a different pattern of sub-surface damage. The study clarifies the applicability of the BIT and offers a useful guideline for practitioners.

Keywords: Hertzian indentation; Bonded–interface technique; Alumina; Finite element method

1. Introduction

Analysis of sub-surface damage in a material is important to understand the deformation mechanisms in machining and indentation. For hard and brittle materials such as ceramics, the technique of cross-section view examination is time consuming and difficult to perform. Thus an apparently straightforward method, the bonded–interface technique (BIT) [1–3], has been used by quite a number of research groups to facilitate the analysis of sub-surface damage. The BIT uses two relatively square and equally shaped samples of the same material. A surface on each sample is polished and glued together by a cyanoacrylate superglue, as shown in Fig. 1. The glue layer in the

* Corresponding author. + Tel.: 00-61-2-9351-2835; fax: + 00-61-2-9351-7060.
E-mail address: zhang@mech.eng.usyd.edu.au (L. Zhang).

0020-7403/01/$ - see front matter
PII: S0020-7403(00)00032-1

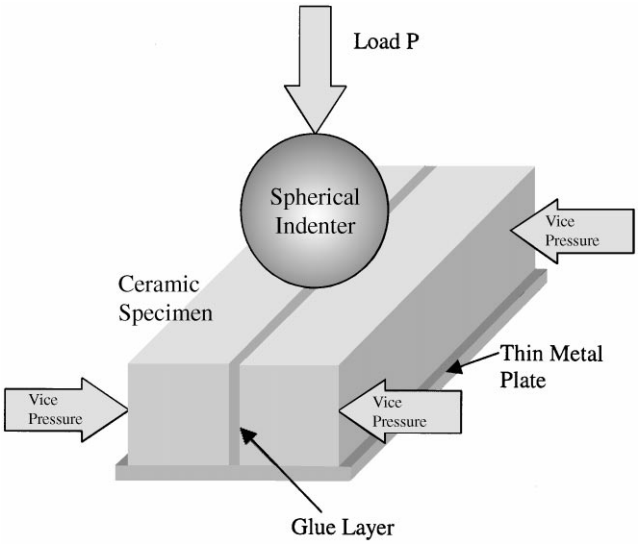

Fig. 1. Schematic of bonded–interface technique.

indented specimen will therefore be resolved chemically and the sub-surface damage induced by the indentation can then be examined conveniently by inspecting the halves of the specimen. However, this method violates the axisymmetric, continuous and homogeneous conditions on which the analytical Hertzian stress field is based. It is claimed that if the glue layer thickness is small enough the above inconsistence will have a negligible impact on the indentation results, although this view has not been validated in published literature. As such, there exists an argument that the BIT may not really reveal truly damaged zones, because it actually examines a specimen that experiences a non-identical stress field compared to a real workpiece, leaving a legitimate concern about the conclusions of material characterisations drawn from samples prepared with the bonded–interface technique.

This study intends to clarify the applicability of the BIT by a systematic finite element stress analysis, and a comparison with a corresponding experiment. Since indentation was the test that first introduced the BIT, the present study will focus only on the analysis of indentation.

2. Finite element modelling and experimentation

The choice of indenter size, loading conditions, and specimen material (alumina) for this study are based on a paper by Guiberteau et al. [1] who first introduced the BIT. The term bonded–interface in this study refers to a specimen prepared using the BIT, or a finite element model that has a glue layer. Conversely, the term integral refers to a specimen or a finite element model that represents a continuous, homogeneous material subjected to a standard Hertzian indentation. It is clear that the deformation of an integral specimen is axisymmetric, while that of the bonded–interface specimen is only symmetric about the central plane of the glue layer (*XZ*-plane) and the *YZ*-plane, as shown in Fig. 2. Also seen in Fig. 2 are the boundary conditions of the FE model, and the terminology used in this study.

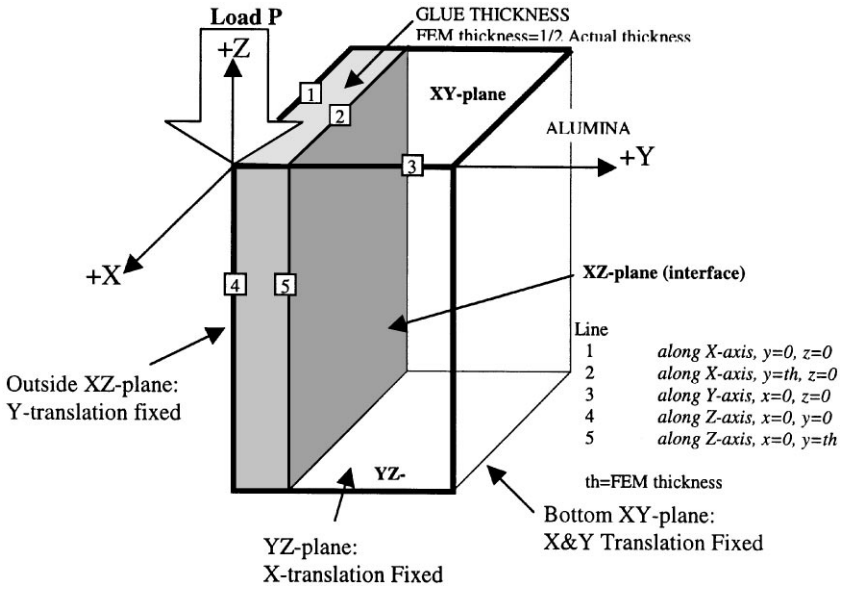

Fig. 2. Schematic of lines and planes analysed in 3-D model.

The finite element (FE) model for both the elastic and elastic–plastic analyses are shown in Fig. 3a and b. Due to the symmetry outlined above, only a quarter of a specimen is needed for analysis. Fig. 3a is a finite element model created by a revolved surface mesh which gives a natural correspondence of nodes in the indenter and the specimen. The bonded–interface model is created by adding a glue sheet of elements to the left side of the cylindrical model, as illustrated in Fig. 3b. The elements in this sheet are arranged in the same mesh configuration, so that nodes in the glue layer correspond to those in the alumina body. The smallest control volume was determined to be 800 μm (radius) × 1200 μm (height) with which the normal stress distribution on the bottom surface of the specimen became uniform and the normal and shear stresses on its peripheral surface vanished. Hence, the boundary effect was eliminated. With the 27-node solid elements, the verification of the mesh size showed that a further increase of the number of elements from 1328 did not significantly improve the correlation of the finite element model with the analytical solution of Hertzian indentation [4], as shown in Fig. 3c. This resulted with 1328 elements in the cylinder and an addition of 332 elements for the glue layer and brought the bonded interface model element count to 1660. The contact between the indenter and the specimen was treated by the segment method of the ADINA code [5] which used Lagrange multipliers to enforce the contact conditions with the kinematic conditions being enforced at the contactor nodes and the frictional conditions enforced over the contact segments.

The spherical indenter, with a radius of 3.18 mm, was modelled as a rigid 3-D surface. The contact pressure, p_m, was set to 8 GPa to match the experimental condition specified by Guiberteau, et al. [1]. For the elastic–plastic analysis, the mechanical properties of alumina were assumed to follow the Von Mises yield criterion and its associated flow rule with linear

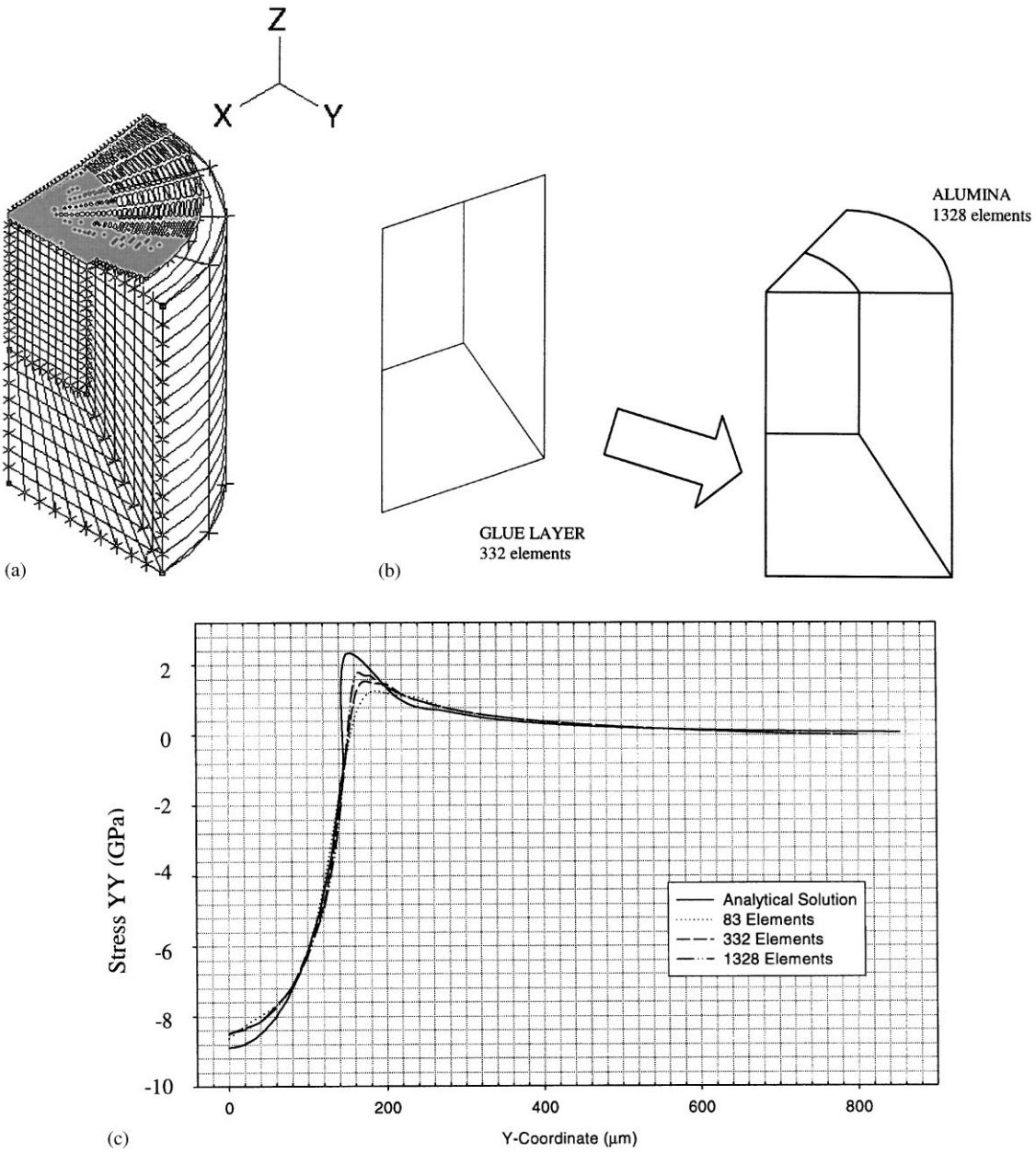

Fig. 3. Finite element modelling: (a) 3-D finite element model; (b) schematic of 3-D bonded-interface model; (c) effect of mesh size on the radial stress along Y-axis ($x = 0$, $z = 0$).

work-hardening. In this case, the glue layer properties and thickness were kept constant. The elastic–plastic model was validated by fitting the FE indentation stress–strain curve ($p_m \propto a/R$) with the experiment.

Table 1
Thickness of the glue layer (μm) used in the finite element BIT models when with different Young's modulus and Poisson's ratio

Young's modulus (GPa)	Poisson's ratio				
	0.25	0.30	0.35	0.40	0.45
0.10	5	5	5	5	5
0.80	5	3/5/10	5	3/5/10	5
1.50	5	1/3/5/10	5	3/5/10	5
2.20	5	5	5	5	5
	Glue layer thickness (μm)				

In the experimental investigations, both the integral and BIT specimens were prepared from the 25 μm-grained alumina with Young's modulus $E = 393$ GPa and Poisson's ratio of $v = 0.22$. The sample preparation procedure was as follows. Samples of $50 \times 20 \times 5$ mm were polished on the precision polishing machine PL50 with loose diamond abrasives (mean diameters of 15, 6 and 1 μm, respectively). The average surface roughness achieved was 0.1 μm and surface flatness 0.8 μm. A cyanoacrylate superglue was then applied to bond the two polished samples together. A small hand vice was used to exert pressure on the glue faces to ensure a thin bond layer. The glue was cured at room temperature in 24 h and then the bonded specimen was glued to a thin metal plate, keeping the bond layer perpendicular to the metal plate, as shown in Fig. 1. The top surface that indentation would be carried on was polished again in the same manner as specified above. The experimental bond thickness was measured to be between 3 and 5 μm, prior to indentation and the quality of the initial bonding was checked by means of scanning electron microscope to ensure that no bonding defect existed.

The indentation experiment was done on an Instron Universal Testing Machine, model 8501 with a 5 kN load cell, which is capable of controlling both the displacement and maximum load. The indentation was done at the loading speed of 10 μm/s with a tungsten carbide (WC) indenter of radius 3.2 mm, Young's modulus (E) 614 GPa and Poisson's ratio (v) 0.22. Mostly the maximum indentation load of 2000 N was selected so that the contact pressure of $p_m \approx 8$ GPa was obtained. To understand the effect of the maximum indentation load on the nature of subsurface damage, however, additional experiments with the maximum load of 2500 N was also conducted. Six indentations were done under each identical loading conditions. Table 1 summarises the various permutations of Young's modulus, Poisson's ratio and bond thickness that are examined in the present elastic analysis. The elastic–plastic analysis was done at a glue thickness of 5 μm with $E = 1.5$ GPa, and $v = 0.30$.

3. Results and discussion

The differences in the integral and BIT specimens revealed by the elastic-plastic finite element analysis show a very similar nature to those of the elastic deformation in terms of both the

variations of stresses and displacements. This is because under the given indentation load the plastic deformation zone in a specimen is small and is fully restrained by the surrounding elastic zone. Therefore, in the following, the discussion on the finite element analysis will focus on the results of elastic deformation.

3.1. Displacement

The displacement analysis at the alumina interface edges, along the surface and along the negative Z-axis (lines 2 and 5 in Fig. 2), reveals both the role of the glue mechanical properties, and a major effect of the BIT. Illustrated in Fig. 4 are the X, Y and Z displacements for various mechanical properties of the glue layer along these two edges. The glue layer mechanical properties shown include the extremes of the permutations of Young's modulus and Poisson's ratios listed in Table 1, and are the limits of the bonded–interface model behaviour. It can be seen from the two graphs that X- and Z-displacements are not greatly affected by the bonded–interface or the mechanical properties of the glue layer. This is highlighted by the overlapping displacement curves of the various models displayed. It should be noted that the models are in the second quadrant of the XY plane, and so the positive X-displacements indicate that the alumina is being drawn towards the load centre.

The Y-displacements, on the other hand, show behaviour very much dependent on the mechanical properties of the bonded–interface. As expected, the glue layer offers little support to the alumina edge, allowing considerable displacement in the negative Y direction. The stronger the glue layer material, the greater the support, and the less the displacement. Experiments done in the course of this study have placed the Young's modulus of the cyanoacrylate glue around 1.2 GPa. Considering that of the glue layer material ranged from 0.1 to 2.2 GPa, it can be seen that the glue properties do not have a significant effect on the general behaviour of the bonded–interface model.

3.2. Stress

The results of the elastic FE analysis show that a distinctive stress field is associated with the BIT that is sufficiently different from the normal Hertzian stress field. For the range of glue mechanical properties analysed, it has been found that the glue has a minimal effect on this general behaviour.

Shown in Fig. 5 is the maximum shear stress comparison on the central plane of the glue layer (XZ-plane). It can be seen that the stress levels in the glue layer are significantly less than those found in the integral model where the specimen is a continuous alumina. As well, the normal sub-surface Hertzian stress field is not maintained. This indicates that the glue layer not only breaks the continuity of the alumina, but in effect produces almost free surfaces on the interface planes. Since free surfaces attract dislocations by their ability to reduce dislocation energy [6], it is expected that both dislocation and crack propagation behaviour would be affected, and a difference in sub-surface damage observable between indentation of integral alumina specimens, and BIT ones. Another concern with the glue layer is its ability to withstand the shearing forces that are being applied. Under the best bonding conditions, the cyanoacrylate glue can take 26 MPa of shear stress [7]. In an area greater than that shown in Fig. 5, namely 800 μm wide and 250 μm deep, a total failure of the glue is expected. These conclusions are confirmed in the experimental comparison presented later in this paper.

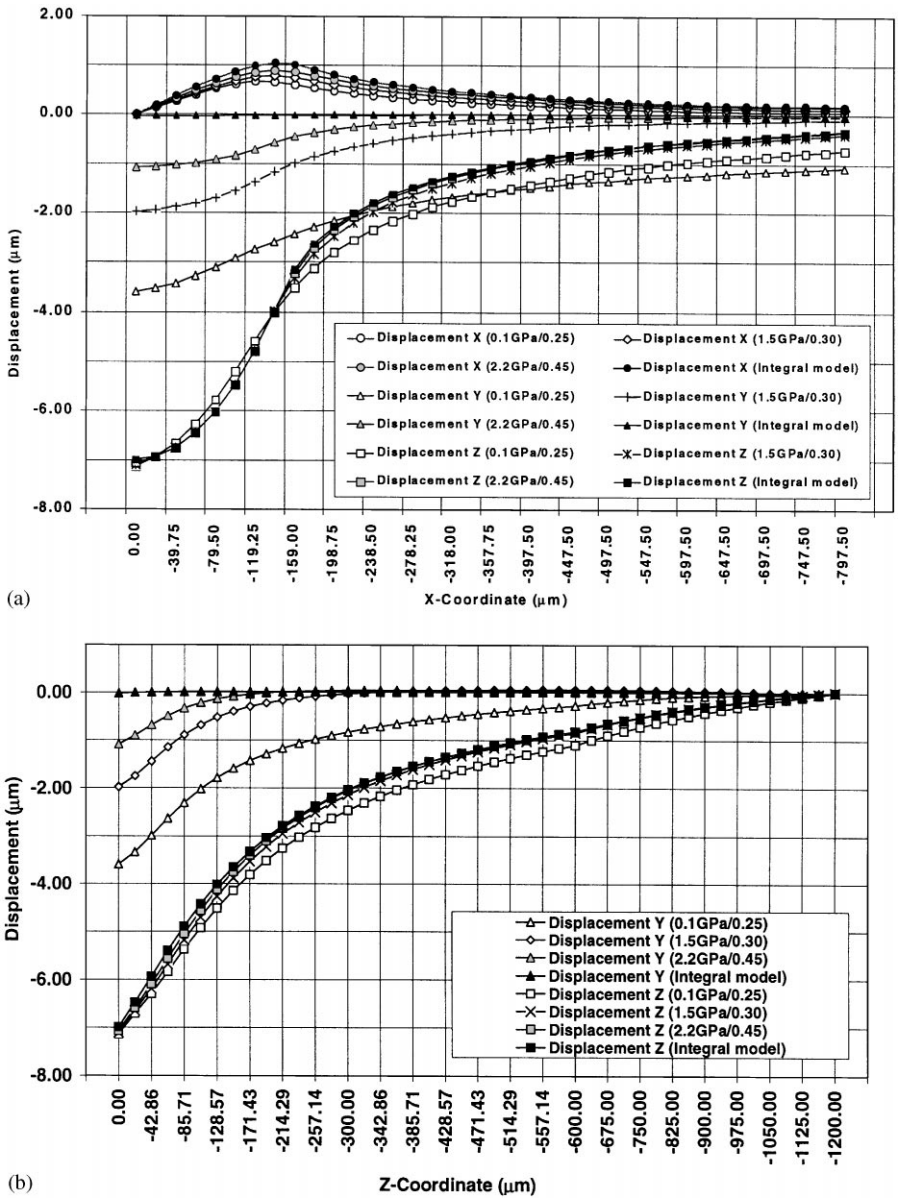

Fig. 4. Effect of glue properties (Young's modulus/Poisson's ratio) on displacement in X, Y, and Z directions: (a) $z = 0$ along line 2 defined in Fig. 2; (b) $x = 0$ along line 5 defined in Fig. 2.

Shown in Fig. 6 are the effective stress curves for the X- and Z-axis interface edges and the line along Y-axis (lines 2, 5 and 3 in Fig. 2). These graphs highlight the limited role of the glue layer mechanical properties on the overall behaviour of the bonded–interface model. It can be seen that the influence of the BIT on the stress distribution is primarily in the vicinity of the indentation surface. This is most clearly seen in Fig. 6b, where the glue properties show their greatest effect in

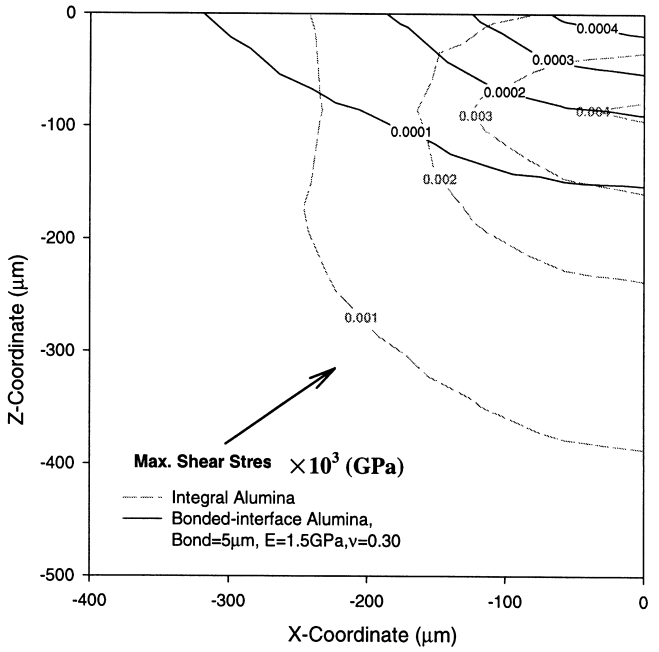

Fig. 5. Maximum shear stress distribution on the central plane of the glue layer ($y = 0$) in BIT and that on the central plane ($y = 0$) of the integral alumina.

the top 20 μm. With increasing depth, both models follow parallel profiles, and the effect becomes negligible. This is reasonable since the alumina is subject to more constraints, along its depth than on the surface. The relatively high effective stresses on the surface can be seen in Fig. 6c. While the integral model shows a progressive reduction in the stress level, the bonded–interface models experience a rapid peaking in stresses within the first 40 μm from the indenter centre, followed by a drop that, although rapid, does not converge with the integral model. The dip in the curves around the 140 μm Y co-ordinate is a function of the errors of the transition from compressive stresses under the indenter, to the tensile stresses outside. Another peculiar behaviour can be seen from Fig. 6a, where four bonded–interface curves having $E = 0.10$ GPa deviate from the normal BIT behaviour. This is explained by the fact that when the glue layer is sufficiently soft and cannot resist the Y-displacements of the alumina, the interface edge of the alumina on one side of the glue layer will eventually meet its counterpart on the other side. The interference of these harder alumina edges will resist further displacements, which results in the build-up of effective stresses.

The effective stress contours are shown in Fig. 7 for 3 planes of interest. Fig. 7a shows the cross-sectional view of the BIT model (YZ-plane). Fig. 7b shows the indentation surface (XY-plane), and Fig. 7c shows the bonded–interface plane (XZ-plane). The bond thickness examined is 5 μm, and the glue layer properties are $E = 1.5$ GPa and $v = 0.30$, to be in range with experimental expectations. It can be seen from Fig. 7a that the high sub-surface stress field in the bonded–interface model is shifted away from the load centre, into the body of the specimen. This can be explained by the following. When the interface edge is allowed to collapse into the glue layer,

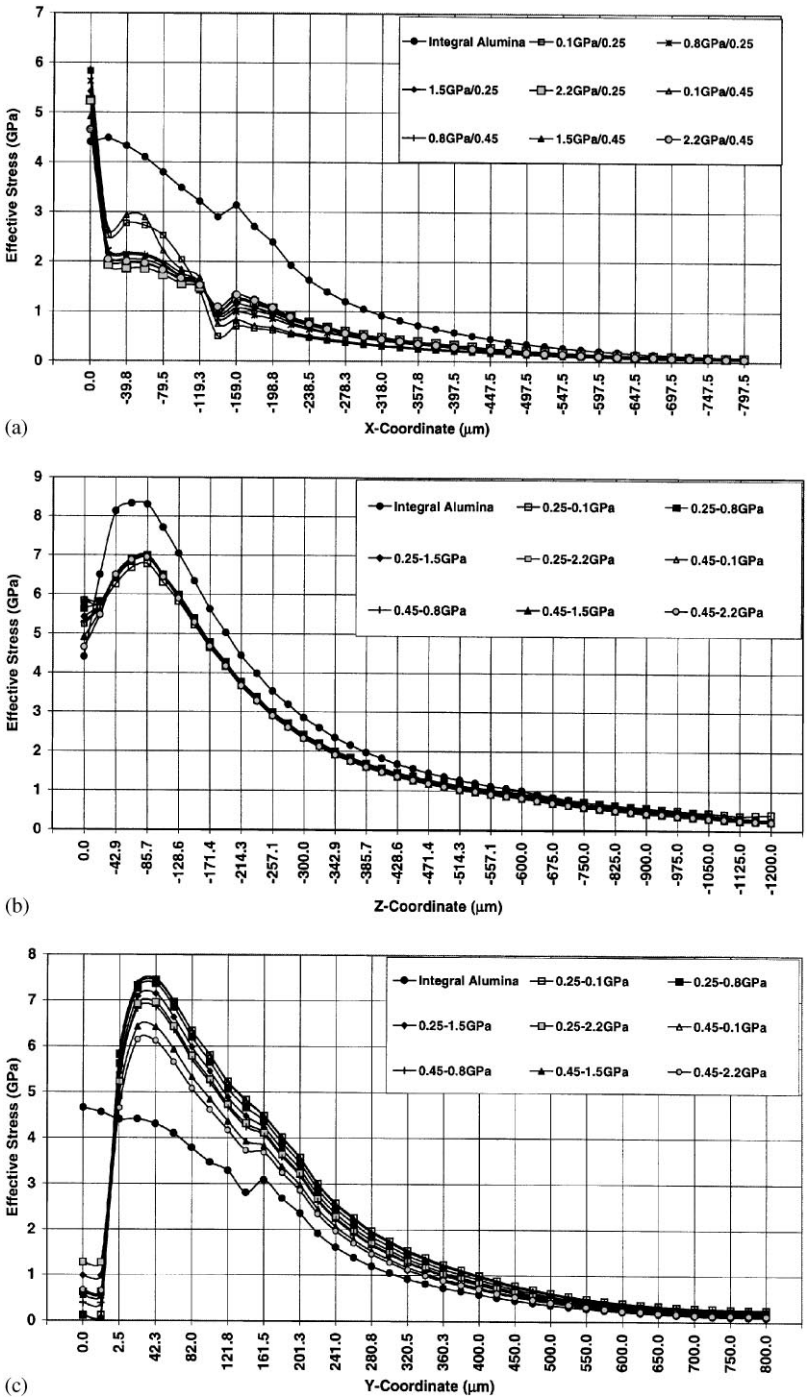

Fig. 6. Effect of glue properties (Young's modulus/Poisson's ratio) on effective stress distribution: (a) along X-axis alumina interface at $y = 2.5\,\mu\text{m}$, $z = 0$; (b) along Z-axis alumina interface at $y = 2.5\,\mu\text{m}$, $x = 0$; (c) along Y–axis edge at $x = z = 0$.

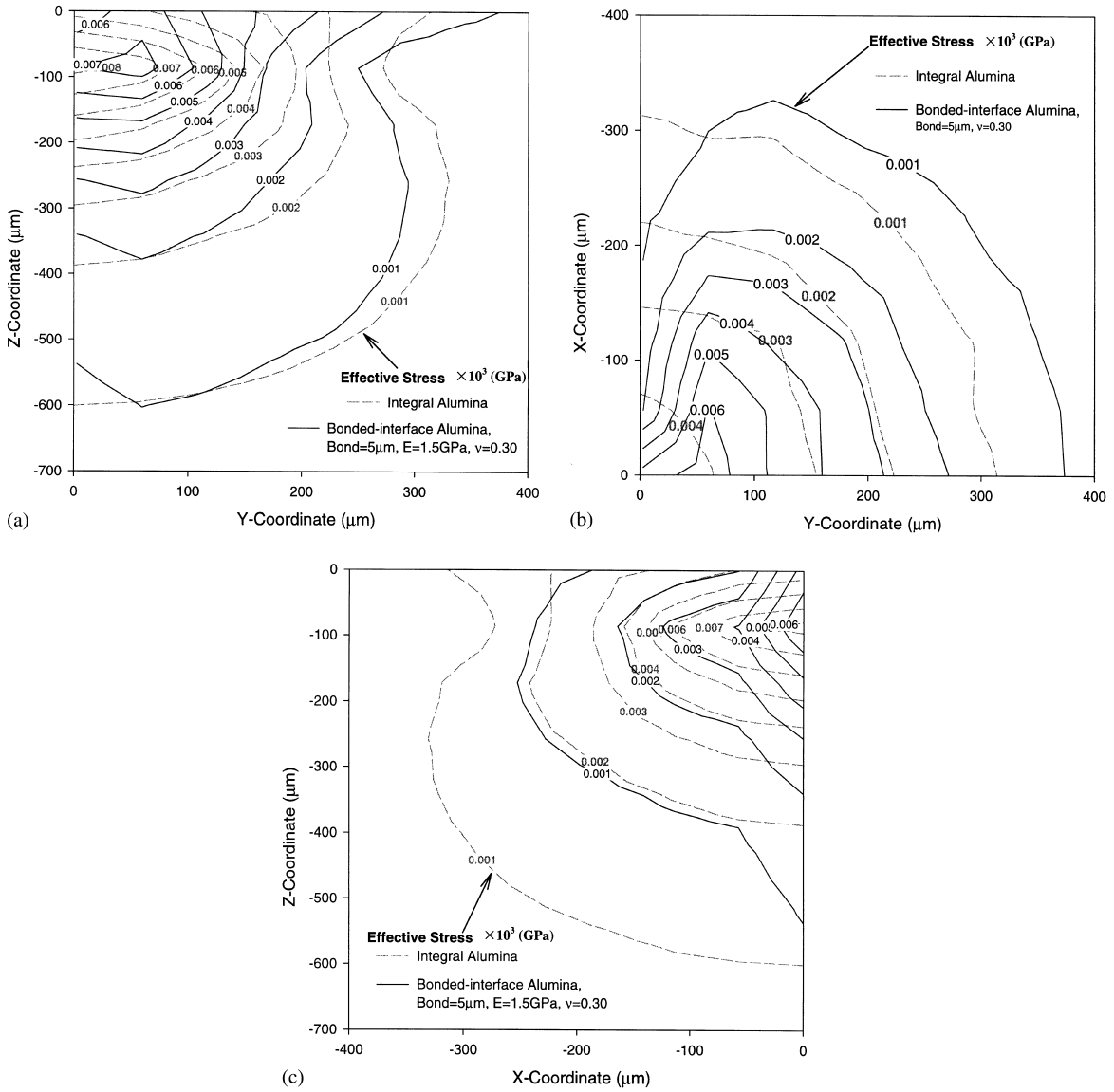

Fig. 7. Effective stress distribution in BIT and integral alumina: (a) in *YZ*-plane; (b) in *XY*-plane; (c) in *XZ*-plane.

a shift occurs in the major point of contact between the alumina and the indenter. In the integral model, the major contact point is directly below the centreline of the indenter, and radiates axisymmetrically outward. In the bonded–interface models, the centreline of the indenter is over the glue, which as shown, cannot support the indenter adequately. As the load increases, the interface edge collapses, and leads to a corresponding shift of the maximum stress field away from the bonded-interface. As well, the high-stress field is no longer contained in the sub-surface region, but extends to the surface, where they are significantly higher for the BIT model. This is clearly seen in Fig. 7a and b. Using an effective yield stress of around 4.2 GPa, it can be seen that overall, the

sub-surface damage zone is expected to be greater in the integral alumina, while the BIT alumina will suffer additional damage on the surface. These are confirmed by experimental investigations to be presented later.

Another effect found in the BIT model is a stress concentration along the *Z*-axis interface edge, on the *XZ*-plane, and shown in Fig. 7c. This is consistent with the high *Y*-displacements on this edge seen in Fig. 4b, and has a short-lived effect. As the distance from this large displacement increases, the stress field reverts to the Hertzian profile. Again, consistent with the shifted stress field, the overall stresses on this plane are lower; however, damage related to the high displacements along this stress concentration is expected.

3.3. Experimental investigation

The experimental results are consistent with the conclusions drawn from the above analysis. The effect of the variation of the maximum indentation load lies in that the sizes of the damaged zones in specimens varies. Since the nature of the results from the two indentation loads is the same, only those corresponding to 2000 N are presented in detail below.

Fig. 8 shows the residual damage on the surface of both the integral and BIT alumina at the indentation load of 2000 N. It can be seen that a significant difference exists in the extent of the damage experienced by each specimen. A scanning electron microscope (SEM) close-up in Fig. 9 shows that individual grains in the BIT alumina have been rearranged randomly in a manner consistent with high displacements. The experimental bonded–interface alumina tends to favour damage along the interface edge, creating a slightly oval profile, which is not seen in the FE analysis. This can be accounted for by the fact that the finite element analysis does not consider either grain size effect or friction, and assumes that alumina behaviour on the bonded–interface surface is the same as within the bulk of the material. Since the grain size of 25 μm is relatively substantial, grain dislodgement would be quite easy in high-stress areas. With the interface edge

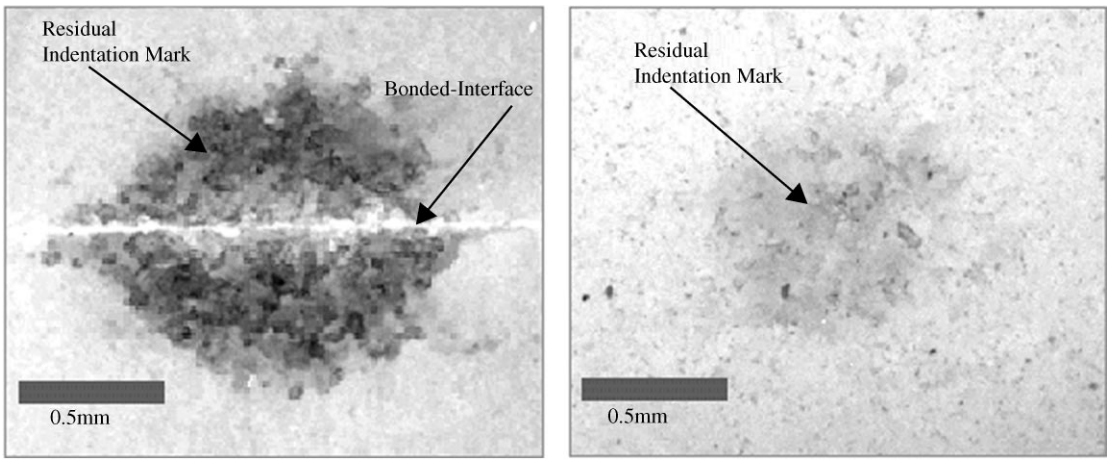

Fig. 8. Surface topography of alumina: (a) bonded–interface; (b) integral.

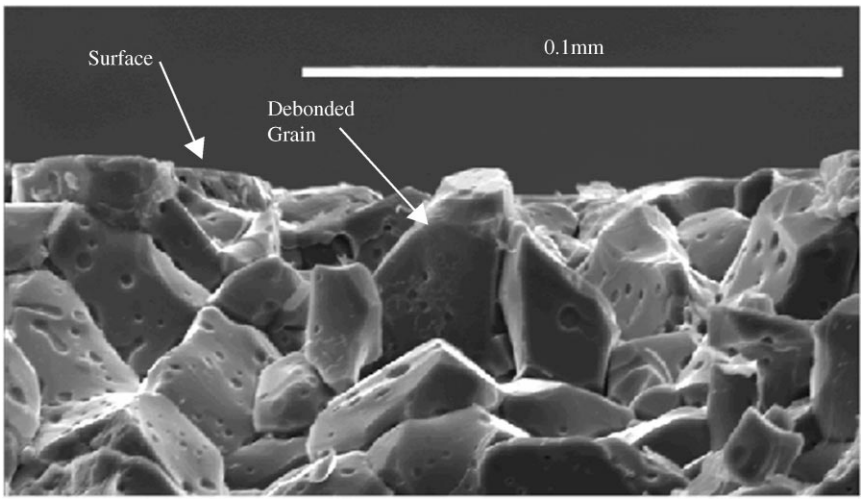

Fig. 9. Surface topography of the bonded–interface alumina at higher magnification.

unsupported by the glue layer over its whole length, weaker grain boundaries and friction would have a more obvious effect there than within the bulk of the material.

The glue layer's inability to support the interface edge and withstand the high stress field of indentation, predicted by the elastic analysis, is highlighted in Fig. 10, which shows a close-up of the damage created in the cyanoacrylate glue layer. Cracking in the glue layer is obvious, as is the debonding of the alumina interface from the glue. This debonding, which was not considered in the finite element analysis, would be an added source of variation between the experimental behaviour and finite element behaviour. It can also be noted that the original bond thickness of around 5 μm has increased. This can be explained by the fact that, in actual indentation, the large irreversible deformations would not allow the two alumina halves to return to their original positions once the load is removed, especially since debonding occurs at the glue-alumina interface.

From Fig. 11a, showing the damage on the BIT interface plane (*XZ*-plane), and Fig. 11b showing the cross-sectional view of the integral alumina plane (*XZ* and *YZ*-plane), both at the indentation load of 2000 N, it can be seen that the nature of the damage is markedly different in each specimen. Overall, the damage zone is about 30% deeper in the integral specimen, but the damage is localised in clusters where the intergranular boundary strength is weaker and undamaged grain boundaries could be located easily. No dislodgment of grains was detected. In contrast, the BIT alumina, experiences more complete damage in the high stress zone, and extends to the surface more perceptibly than in the integral alumina. It is characterised by a high density of cracks running between the grains which were almost separated and easily dislodged from the BIT surface (Fig. 11a). Also, the damage zone favours the Z-axis centreline, as was seen by the stress concentration in Fig. 7c. SEM close-ups of this interface plane reveal random grain rearrangement, intergranular and transgranular cracking, and slip lines, all consistent with high levels of plastic deformation and displacements. The similarity of this damage with the surface damage highlights the almost free surface behaviour expected on the interface plane.

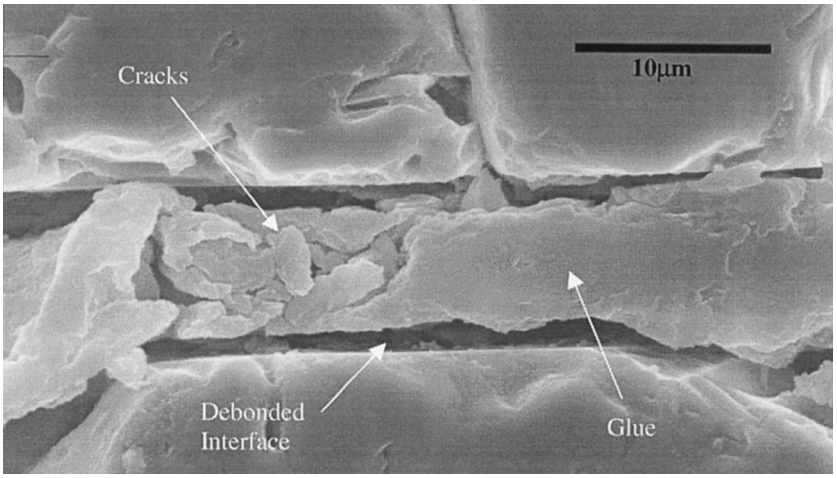

Fig. 10. General view of the glue layer after indentation. Note the debonding at the glue–alumina interface.

Finally, Fig. 11c illustrates a cross-sectional view of the BIT alumina (*YZ*-plane) at the indentation load of 2000 N. Within the bulk of the material, the nature and area of the damage is more consistent with that seen in the integral alumina. On approaching the interface plane, the damage is with heavily deformed and dislodged grains. It is also evident that the damaged zone in the bulk material is deeper than on the interface plane. Again, this is consistent with the FE analysis (Fig. 7a), which predicted a deeper damage in the bulk.

4. Conclusions

From this study, several conclusions can be obtained:

(1) The BIT model experiences a different, non-axisymmetric stress field than that of the normal Hertzian indentation. Whereas the integral model encounters the highest stresses in the sub-surface region, the BIT model has relatively high stresses on the surface. The BIT model will also experience high sub-surface stress, but the stress field is shifted into the body of the alumina, and away from the bonded–interface. For a given indenter displacement, the bonded–interface will register lower overall stresses within the alumina body. The relatively high surface stress, the shifted stress field, and the lower overall stresses within the alumina body, all result from loss of material continuity and the glue layer's inability to support the interface plane near the surface. This lack of support from the glue translates to significant horizontal *Y*-displacements of the interface edges, which in turn rearranges the nature of contact between the indenter and the alumina specimen. The type of resulting damage is also closely related to high displacements.
(2) Within the realistic range of mechanical properties of the cyanoacrylate glue, the glue properties have a limited effect on the behaviour of the bonded–interface model. In addition, since the

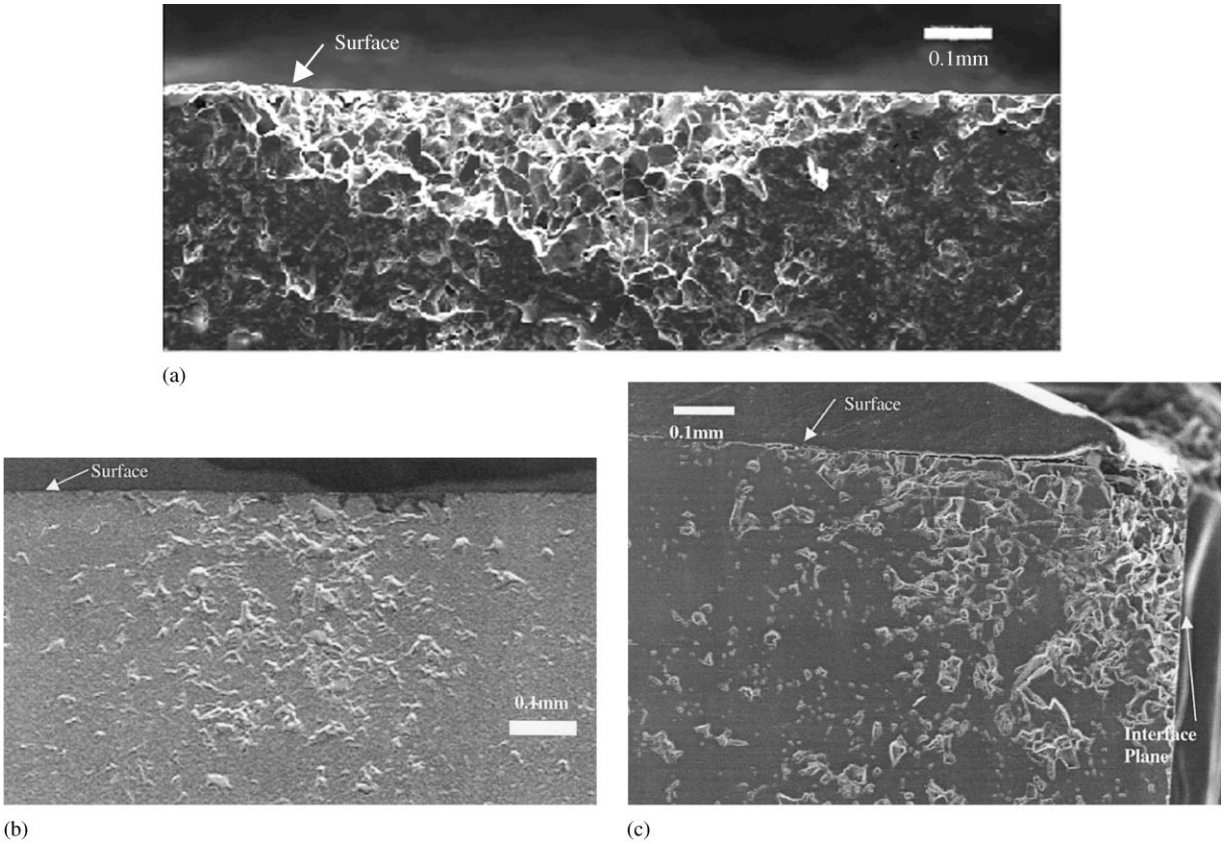

Fig. 11. Subsurface damage: (a) on *XZ* plane of the BIT alumina; (b) on *XZ*-plane of integral alumina; (c) on *YZ*-plane of the BIT alumina.

stresses experienced by the glue layer are much higher than its material strength, it is expected that the glue layer will break, modifying, to a degree, the behaviour seen in this bonded-interface analysis.

(3) Bond thickness has a minimal effect on the general behaviour of the bonded–interface model.
(4) From the practical point of view the subsurface damage zone created in BIT alumina is characterised by more severe damage and smaller depth of penetration in comparison with integrated alumina.
(5) The BIT cannot reveal the true nature of sub-surface damage in hard and brittle materials such as alumina.

Acknowledgements

The authors wish to thank Dr. T. Liu and Dr. B. Latella from ANSTO Australia for assistance in preparation of BIT samples and running the indentation experiments. Thanks are also due to the Electron Microscope Unit of Sydney University for use of its facilities.

References

[1] Guiberteau F, Padture NP, Lawn BR. Effect of grain size on hertzian contact damage in alumina. Journal of the American Ceramic Society 1994;77:1825–31.
[2] Lawn BR, Panture NP, Guiberteau F, Cai H. A model for the micro-crack initiation and propagation beneath hertzian contacts in polycrystalline ceramics. Acta Metalurgica Materialia 1994;42:1683–93.
[3] Latella BA, O'Connor BH, Padture NI, Lawn BR. Hertzian contact damage in porous alumina. Journal of the American Ceramic Society 1997;80:1027–31.
[4] Johnson KL. Contact mechanics. Cambridge, UK: Cambridge University Press, 1985.
[5] ADINA R&D Inc., Theory and modelling guide, vol. I: ADINA. USA: ADINA R&D, Inc., USA.
[6] Green DJ. An introduction to the mechanical properties of ceramics. Cambridge: Cambridge University Press, Cambridge, UK, 1998.
[7] Development & Engineering Group of Loctite Research. Technical data sheet: product 401, Dublin, Ireland, 1996.